ORIGINAL ARTICLE

Rapid detection of the *MYD88* L265P mutation for pre- and intra-operative diagnosis of primary central nervous system lymphoma

Junya Yamaguchi[1] | Fumiharu Ohka[1] | Yotaro Kitano[2] | Sachi Maeda[1] | Kazuya Motomura[1] | Kosuke Aoki[1] | Kazuhito Takeuchi[1] | Yuichi Nagata[1] | Hikaru Hattori[3] | Takashi Tsujiuchi[4] | Ayako Motomura[4] | Tomohide Nishikawa[1] | Yuji Kibe[1] | Keiko Shinjo[5] | Yutaka Kondo[5] | Ryuta Saito[1]

[1]Department of Neurosurgery, Nagoya University Graduate School of Medicine, Nagoya, Japan

[2]Department of Neurosurgery, Mie University Graduate School of Medicine, Tsu, Japan

[3]Department of Medical Genomics Center, Nagoya University Hospital, Nagoya, Japan

[4]Department of Neurosurgery, Daido Hospital, Nagoya, Japan

[5]Division of Cancer Biology, Nagoya University Graduate School of Medicine, Nagoya, Japan

Correspondence
Fumiharu Ohka, Department of Neurosurgery, Nagoya University Graduate School of Medicine, 65 Tsurumai-cho, Showa-ku, Nagoya 466-8550, Japan.
Email: fohka@med.nagoya-u.ac.jp

Abstract

The *myeloid differentiation primary response gene 88* (*MYD88*) L265P mutation is a disease-specific mutation of primary central nervous system lymphoma (PCNSL) among the central nervous system tumors. Accordingly, this mutation is considered a reliable diagnostic molecular marker of PCNSL. As the intra-operative diagnosis of PCNSL is sometimes difficult to achieve using histological examinations alone, intra-operative detection of the *MYD88* L265P mutation could be effective for the accurate diagnosis of PCNSL. Herein, we aimed to develop a novel rapid genotyping system (GeneSoC) using real-time polymerase chain reaction (PCR) based on microfluidic thermal cycling technology. This real-time PCR system shortened the analysis time, which enabled the detection of the *MYD88* L265P mutation within 15 min. Rapid detection of the *MYD88* L265P mutation was performed intra-operatively using GeneSoC in 24 consecutive cases with suspected malignant brain tumors, including 10 cases with suspected PCNSL before surgery. The *MYD88* L265P mutation was detected in eight cases in which tumors were pathologically diagnosed as PCNSL after the operation, while wild-type *MYD88* was detected in 16 cases. Although two of the 16 cases with wild-type *MYD88* were pathologically diagnosed as PCNSL after the operation, *MYD88* L265P could be detected in all eight PCNSL cases harboring *MYD88* L265P. The *MYD88* L265P mutation could also be detected using cell-free DNA derived from the cerebrospinal fluid of two PCNSL cases. Detection of the *MYD88* L265P mutation using GeneSoC might not only improve the accuracy of intra-operative diagnosis

of PCNSL but also help the future pre-operative diagnosis through liquid biopsy of cerebrospinal fluid.

KEYWORDS
cfDNA, liquid biopsy, MYD88, primary central nervous system lymphoma, rapid diagnosis

1 | INTRODUCTION

Primary central nervous system lymphoma (PCNSL) is a form of malignant lymphoma that arises from the central nervous system (CNS), such as the brain parenchyma, spine, or eyes (ocular lymphoma). Most PCNSLs exhibit histological features of diffuse large B cell lymphoma (DLBCL). PCNSL accounts for 3%–4% of malignant CNS tumors; however, its incidence has been increasing in the past decade, especially in elderly people. The standard treatment strategy for PCNSL is the immediate introduction of chemotherapy, including high-dose methotrexate (HD-MTX) and radiation therapy. A pivotal subject of tumor removal surgery for PCNSL involves the collection of the tumor tissue for pathological diagnosis. In contrast, the maximal extent of tumor resection is quite important for the favorable prognosis of diffuse infiltrative glioma. Intra-operatively distinguishing between these tumors based on pathological findings is frequently difficult. Accordingly, intra-operative decision-making for the extent of tumor removal is also difficult. Overall, it is important to detect various characteristic molecular features that might be important for tumor diagnosis pre-operatively and intra-operatively.

Based on comprehensive genome analysis, gene mutations related to the NFkB pathways are enriched in PCNSL. Notably, the *myeloid differentiation primary response gene* (*MYD88*) mutation is detected in approximately 70% of PCNSL cases, which is higher than that of systemic DLBCL cases.[1-7] The *MYD88* mutation is a recurrent hotspot (L265P) mutation. Furthermore, the *MYD88* L265P mutation is rarely detected in other types of brain tumors[8-11] and is reported to be a potential reliable diagnostic molecular marker of PCNSL.[12-14] The *MYD88* L265P mutation has been successfully detected using gDNA derived from tissue samples and cell-free DNA (cfDNA) derived from cerebrospinal fluid (CSF) or plasma.[12-14] Droplet digital polymerase chain reaction (ddPCR) and Sanger sequencing are the primary technologies used to detect the *MYD88* L265P mutation in previous studies. As these methods require more than a few hours to detect the *MYD88* L265P mutation, a novel analysis method that can rapidly detect a small amount of the *MYD88* L265P mutation for accurate pre- and intra-operative diagnosis of PCNSL is warranted.

In this study, we aimed to develop a novel rapid and highly sensitive detection system for the *MYD88* L265P mutation using microfluidic thermal cycling technology, which ultimately enabled the detection of the *MYD88* L265P mutation within 15 min. This system could not only support rapid and accurate intra-operative diagnosis of PCNSL but also help future pre-operative diagnosis by liquid biopsy of CSF.

2 | MATERIALS AND METHODS

2.1 | Patient characteristics

Twenty-four consecutive cases with suspected malignant brain tumors, including 10 cases with suspected PCNSL before surgery, were employed for the intra-operative detection of the *MYD88* L265P mutation using GeneSoC at Nagoya University Hospital in 2021 and 2022. Frozen tumor tissue samples obtained from patients with PCNSL and treated at Nagoya University Hospital between 2013 and 2020 were used for ddPCR analyses. The study was approved by the Institutional Review Board of Nagoya University (2022–0043). Informed consent was obtained from all patients.

2.2 | gDNA extraction and formalin-fixed, paraffin-embedded tissue samples

For intra-operative analysis, a small piece of tumor tissue taken for intra-operative pathological diagnosis (5–25 mg) was added to a tube containing 50 μL distilled water and minced with a needle. The tube was incubated at 95°C for 5 min to elute gDNA. After brief centrifugation, the supernatant was collected for GeneSoC analysis. To conduct conventional molecular analysis, gDNA was extracted from another piece of the tumor using the QIAamp DNA Extraction Kit (Qiagen) or unstained formalin-fixed, paraffin-embedded (FFPE) using the QIAamp DNA FFPE Kit (Qiagen, Hilden). The concentration of gDNA was determined using Qubit (Thermo Fisher Scientific).

2.3 | cfDNA extraction from cerebrospinal fluid samples

To extract cfDNA from CSF, 10 mL of CSF was collected from ventricles during biopsy surgery before the collection of tumor tissue in Cell-Free DNA BCT CE (Streck, La Vista, USA). Cells were removed via the centrifugation of CSF at 1600×g for 10 min at room temperature. The upper layer of the supernatant was removed and transferred to a new conical tube. Following centrifugation of the CSF at 3200×g for 10 min, cfDNA was extracted using the QIAamp Circulating Nucleic Acid Kit (Qiagen). cfDNA was eluted in 20 μL elution buffer, and its concentration was determined using Qubit (Thermo Fisher Scientific).

2.4 | Detection of the *MYD88* L265P mutation using GeneSoC

Two microliters of the extracted gDNA was mixed with 1 μL of 18 μM primers and 5 μM probes targeting *MYD88* L265P and wild-type (Bio-Rad), 0.8 μL of 0.4 nM Cy5, 1.6 μL of 10 nM dNTP, 2 μL of 10×reaction buffer, 0.5 μL of polymerase, and 12.1 μL of distilled water. For the analysis of cfDNA from CSF, 2 μL of cfDNA from CSF (5 ng/μL) was used. Details of the probes and primers are provided in Table S1. Twenty microliters of the mixed sample was transferred to a cartridge and inserted into the GeneSoC detection unit. PCR was performed using GeneSoC with the following thermal cycling conditions: 50 cycles of denaturation at 94°C for 5 s and annealing and extension at 59°C for 10 s. The process was completed within 15 min. The fluorescent threshold was set to 30 to obtain 100% specificity, and the threshold cycle (Ct) value was determined to be a cycle number exceeding 30 for fluorescent intensity. Therefore, when the FAM fluorescence exceeded 30 within 50 cycles, indicating a Ct value of *MYD88* L265P below 50, a positive mutation was detected. The detail of optimization to set the fluorescent threshold is described in Appendix S1.

2.5 | Droplet digital PCR

Extracted gDNA (10–20 ng) was mixed with 10 μL of 2×ddPCR Supermix for probes (Bio-Rad) and 1 μL of 18 μM primers and 5 μM probes targeting *MYD88* L265P and wild-type (Bio-Rad). Details of the probes and primers are provided in Table S1. Each mixture was combined with 60 μL droplet generation oil (Bio-Rad), and the droplets were generated using the QX200 Droplet Generator (Bio-Rad). PCR was performed on a C1000 Thermal Cycler (Bio-Rad) with the following thermal cycling conditions: 40 cycles of denaturation at 94°C for 30 s, annealing and extension at 53°C for *MYD88* L265P with a ramp rate of 2°C/s for 60 s. The fluorescence intensity of each droplet was calculated using the QX200 Droplet Reader (Bio-Rad) and analyzed using the QuantaSoft droplet reader software (Bio-Rad).

2.6 | Construction of the *MYD88* L265P and wild-type plasmid

A plasmid containing each *MYD88* L265P and wild-type sequence was constructed. The *MYD88* fragment containing each *MYD88* L265P mutation point (c.794T>C) and wild-type were amplified by PCR using gDNA derived from a patient harboring the *MYD88* L265P mutation. The primer sequences are listed in Table S1. The fragments were inserted into multiple cloning sites of pcDNA3.1 (Takara bio).

2.7 | Statistical analysis

The receiver operating characteristic curve and the area under the curve (AUC) were generated using GraphPad PRISM version 9.3.1.
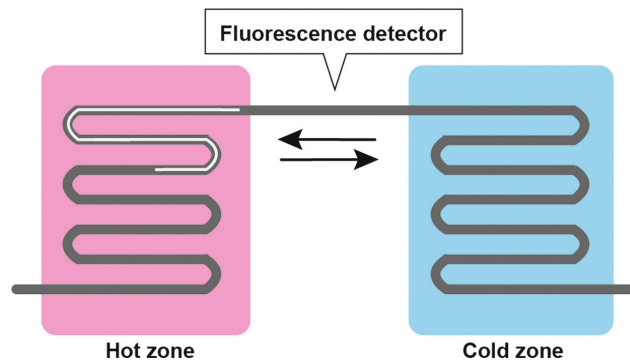
FIGURE 1 Scheme of the microfluidic thermal cycling technology. The reaction mixture moves repeatedly between two temperature zones in a short microchannel.

The *p*-value was determined from the normal distribution (two-tail), assuming an AUC of 0.5. A *p*-value <0.05 was considered to indicate statistical significance.

3 | RESULTS

3.1 | Sensitivity and specificity of rapid genotyping of *MYD88* L265P using GeneSoC

GeneSoC (Kyorin) is a genotyping system based on real-time PCR using microfluidic thermal cycling technology. In this technology, the applied reaction mixture moves repeatedly between two temperature zones in a short microchannel for thermal cycling using microblowers during the progress of a two-step PCR (Figure 1). The mutation detection principle relies on the TaqMan probe technology.[15] Reactions with conventional real-time PCR devices using a Pertier heater require approximately 1 h for completion; however, GeneSoC shortens the thermal cycling time and completes 50 cycles of real-time PCR within 15 min.

To minimize analysis time, we omitted measuring the concentration of the extracted gDNA via the boiling method. If the amount of gDNA was too high, even for wild-type gDNA (100% wild-type gDNA), the FAM fluorescence might exceed the determined threshold of 30. In contrast, if the amount of applied gDNA was too low, the FAM fluorescence of gDNA, including 5% mutated gDNA and 95% wild-type gDNA, might not exceed 30. To solve these problems, we analyzed the higher concentration of DNA plasmids, including 100% wild-type DNA. Even in the 4 pg/μL and 40 pg/μL plasmid (each estimated copy number; 1.2×10^6 copies and 1.2×10^7 copies), more than 30 of FAM fluorescence could not be detected (Figure 2A). Based on this result, when the Ct of wild-type gDNA is more than 24.7, the application of a markedly high concentration of gDNA might not result in a false positive. To determine the lowest amount of applied gDNA for the detection of 5% mutated gDNA, various amounts of the DNA plasmid samples, including 5% mutated DNA and 95% wild-type DNA, were assessed. At least the 4×10^{-2} pg/μL (estimated copy number; 1.2×10^4 copies) DNA was

FIGURE 2 Sensitivity and specificity of genotyping of *MYD88* L265P using GeneSoC. (A) Dot plot showing the max fluorescent intensity of the *MYD88* L265P mutation (FAM) of plasmids containing the *MYD88* wild-type sequence based on increasing concentrations. (B) Dot plot showing the max fluorescent intensity of the *MYD88* L265P mutation (FAM) plasmids containing 5% *MYD88* L265P sequence based on serial dilutions. (C) Genotyping using GeneSoC (left) and ddPCR (right). The upper panel displays the result based on the frozen sample of the PCNSL case, and the lower panel displays the results based on the frozen sample of the glioblastoma case. The pink line in the ddPCR result indicates the threshold (FAM; 4000, HEX; 3000).
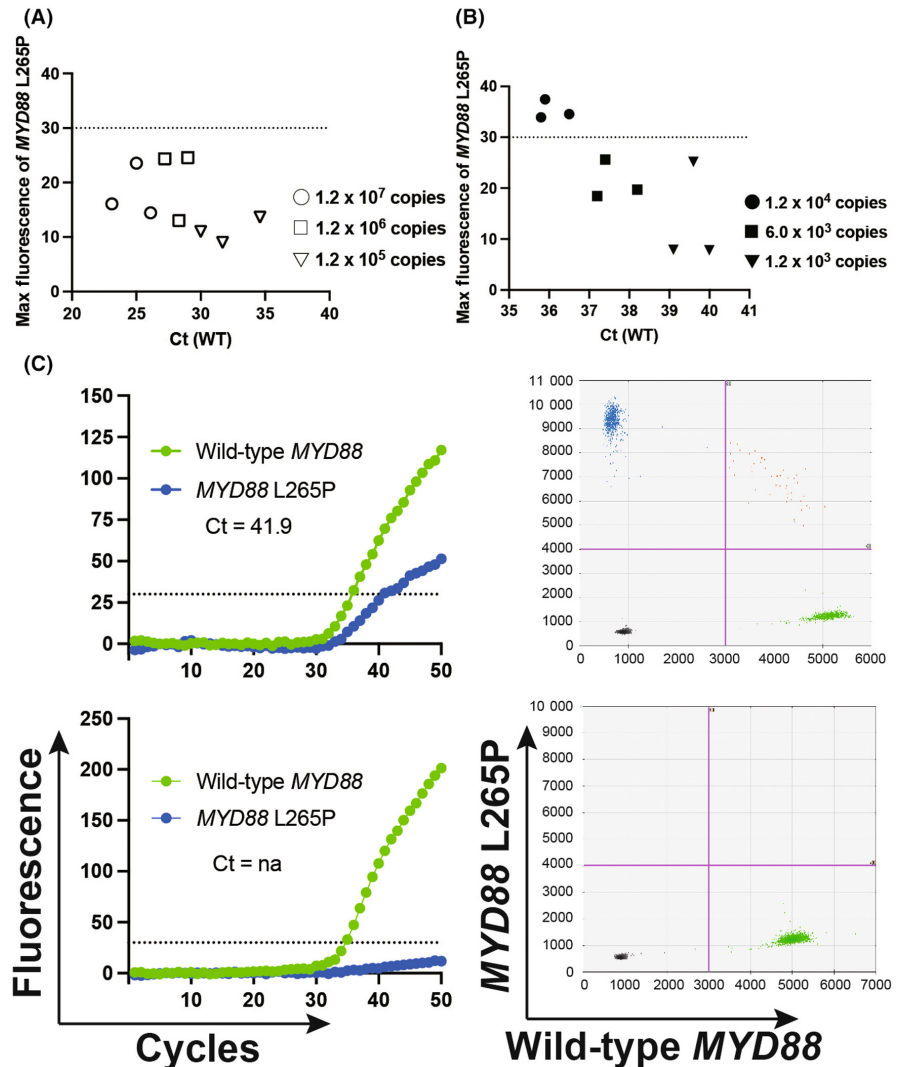
required for the detection of 5% mutated DNA. The Ct of the wild-type DNA in the analysis with the 4×10^{-2} pg/μL (estimated copy number; 1.2×10^4 copies) DNA, including 5% mutated DNA and 95% wild-type DNA, was 36.1 (Figure 2B). Thus, when the Ct of the wild-type gDNA was <36.1, at least 5% of the mutated gDNA could be accurately detected. Based on these findings, genotyping was deemed to be accurately evaluated when the Ct of wild-type *MYD88* (HEX) was between 24.7 and 36.1. To determine the approximate weight of samples for the GeneSoC analysis, the serial weight of frozen tumor samples was analyzed. We found that a minimum of 5 mg of sample was required to obtain the Ct (WT) value within the approximate range (Figure S1d). The variant allele frequency (VAF) of the *MYD88* L265P mutation was detected by ddPCR using gDNA derived from 18 FFPE samples from patients with PCNSL who underwent a biopsy. The median VAF of the *MYD88* L265P mutation of the biopsy sample was 40.1% (Figure S1e). This result indicates that the GeneSoC analysis had enough sensitivity to detect the *MYD88* L265P mutation in biopsy samples.

gDNA derived from a frozen tumor sample of PCNSL exhibiting the *MYD88* L265P mutation via the boil method and glioblastoma as control was analyzed using GeneSoC. The results of GeneSoC

analyses were consistent with those of ddPCR (Figure 2C). Thus, GeneSoC could rapidly detect the *MYD88* L265P mutation with sufficient detection using gDNA derived via the boil method.

3.2 | Intra-operative detection of the *MYD88* L265P mutation using GeneSoC

Under predetermined conditions, genotyping of the *MYD88* gene in 24 consecutive cases of malignant brain tumors was performed intra-operatively. The pathological diagnoses of the 24 cases were DLBCL (*n* = 10), glioblastoma, IDH-wildtype (*n* = 9), astrocytoma, IDH-mutant (*n* = 3), oligodendroglioma, IDH-mutant and 1p/19q codeleted (*n* = 1), and metastatic tumor (*n* = 1). Based on post-operative ddPCR analyses using the same tumor tissue, the *MYD88* L265P mutation was found in eight PCNSL cases, while wild-type *MYD88* was found in 16 cases, including two PCNSL cases. The tumor samples collected during surgery were analyzed using GeneSoC in an operation room. All analyses were completed within 15 min. Among the 10 PCNSL cases, the *MYD88* L265P mutation could be detected in all PCNSL cases exhibiting the *MYD88* L265P

mutation ($n = 8$), while wild-type *MYD88* could be detected in two PCNSL cases exhibiting wild-type *MYD88*. Wild-type *MYD88* could be detected in all non-PCNSL cases ($n = 14$). The characteristics of the 10 PCNSL cases and the 14 non-PCNSL cases are summarized in Table 1 and Table S2. Genotyping of the *MYD88* gene analyzed using GeneSoC revealed consistent results with post-operative ddPCR for all cases. Genotyping using GeneSoC and ddPCR for the representative case (case #2) is shown in Figure 3, and that of the other nine cases is presented in Figure S2. In case #2, sample #1 was collected from the endoscopic entry point, while #2 was collected from an enhanced tumor lesion (Figure 3A). Although the FAM signal was not significantly elevated in sample #1, such elevation was observed in sample #2 (Figure 3B), aligning with the result of post-operative ddPCR (Figure 3C). Consistently, the post-operative pathological diagnosis of sample #2 was DLBCL (Figure 3D).

3.3 | Pre-operative detection of the *MYD88* L265P mutation using cfDNA derived from the cerebrospinal fluid using GeneSoC

The *MYD88* L265P mutation can be detected in cfDNA derived from plasma or CSF.[12–14] The median VAF of the *MYD88* L265P mutation in cfDNA derived from CSF is 17.9% (4.47%–51.7%).[12] We proceeded to verify whether GeneSoC could detect the *MYD88* L265P mutation in cfDNA derived from the CSF. The cfDNA extracted from the CSF of two patients with suspected PCNSL (Case #6 and #10; Figure 4A) was analyzed using GeneSoC. In both cases, the *MYD88* L265P mutation could be detected using cfDNA derived from the CSF, consistent with ddPCR results (Figure 4B,C). The *MYD88* L265P mutation was also detected using gDNA extracted from the biopsy sample.

4 | DISCUSSION

The *MYD88* L265P mutation is a potent disease-specific mutation of PCNSL among CNS tumors. Accordingly, this mutation has been reported as a potential diagnostic molecular marker for PCNSL in gDNA derived from CNS tumors. A highly accurate intra-operative diagnosis can be obtained by combining this diagnostic marker with pathological findings. However, conventional methods, such as Sanger sequencing, require a markedly long time to detect the *MYD88* L265P mutation intra-operatively. In this study, we developed a rapid detection system for the *MYD88* L265P mutation using real-time PCR based on microfluidic thermal cycling technology. Accurate genotyping of *MYD88* could be obtained intra-operatively in 24 cases, including 10 PCNSL cases, using this system. Of note, the volume of tumor samples obtained by biopsy is usually small. Therefore, PCNSL sometimes could not be distinguished from other malignant tumors, including glioblastoma, based on the intra-operative pathological examinations using hematoxylin–eosin staining alone. The accuracy of intra-operative pathological diagnosis of PCNSL is 50–86.9%.[16,17] Additionally, prior use of steroids makes intra-operative pathological diagnosis more difficult to achieve. Repeated correction of tumor samples in biopsy could induce hemorrhagic complications, which might worsen neurological functions and delay the introduction of chemotherapy after surgery.[18] Therefore, several additional diagnostic approaches have been proposed to improve the accuracy of the intra-operative diagnosis of PCNSL. Rapid-immunohistochemistry (R-IHC) for staining CD20 and Ki-67 and intra-operative flow cytometry (iFC) to analyze the aneuploidy of tumor cells are reported to be useful for the intra-operative diagnosis of PCNSL.[17,19] The sensitivity of detecting the *MYD88* L265P mutation for diagnosis of PCNSL has a limit and

TABLE 1 Summary of patients with suspected PCNSL who underwent intra-operative analysis by GeneSoC.

| Case | Sex | Age at diagnosis | Biopsy method | GeneSoC | | | ddPCR | Intra-operative pathological diagnosis | Final diagnosis |
				Ct (WT)	Ct (L265P)	*MYD88* status	*MYD88* status		
#1	F	55	Endoscopic	30.2	31.8	L265P	L265P	na	DLBCL
#2	M	46	Endoscopic	34.4	39.2	L265P	L265P	Malignant tumor (ML suspected)	DLBCL
#3	M	77	Needle	34.6	na	WT	WT	Malignant tumor (ML or metastatic tumor suspected)	DLBCL
#4	M	40	Endoscopic	32.3	39.1	L265P	L265P	na	DLBCL
#5	F	70	Needle	34.7	47.0	L265P	L265P	na	DLBCL
#6	F	80	Endoscopic	32.3	36.6	L265P	L265P	Malignant tumor	DLBCL
#7	M	70	Endoscopic	33.7	39.2	L265P	L265P	Malignant tumor (ML suspected)	DLBCL
#8	F	80	Endoscopic	31.1	na	WT	WT	Malignant tumor (ML suspected)	DLBCL
#9	F	72	Endoscopic	35.9	39.8	L265P	L265P	Malignant tumor (ML suspected)	DLBCL
#10	F	45	Endoscopic	34.3	35.5	L265P	L265P	na	DLBCL

Abbreviations: DLBCL, diffuse large B cell lymphoma; ML, malignant lymphoma; na, not available.

FIGURE 3 Representative clinical case (Case #2). (A) Gd-T1WI of Case #2. (B) Result of GeneSoC for sample #2. The dotted line indicates the fluorescence threshold at 30. (C) Result of post-operative ddPCR for sample #2. The x-axis and y-axis indicate the HEX (*MYD88* wild-type) and FAM (*MYD88* L265P mutation) fluorescent intensity, respectively. The pink line indicates the threshold (FAM; 4000, HEX; 3000) (D) hematoxylin–eosin stain (left) and CD20 stain (right) of sample #2. The scale bar represents 100 μm.
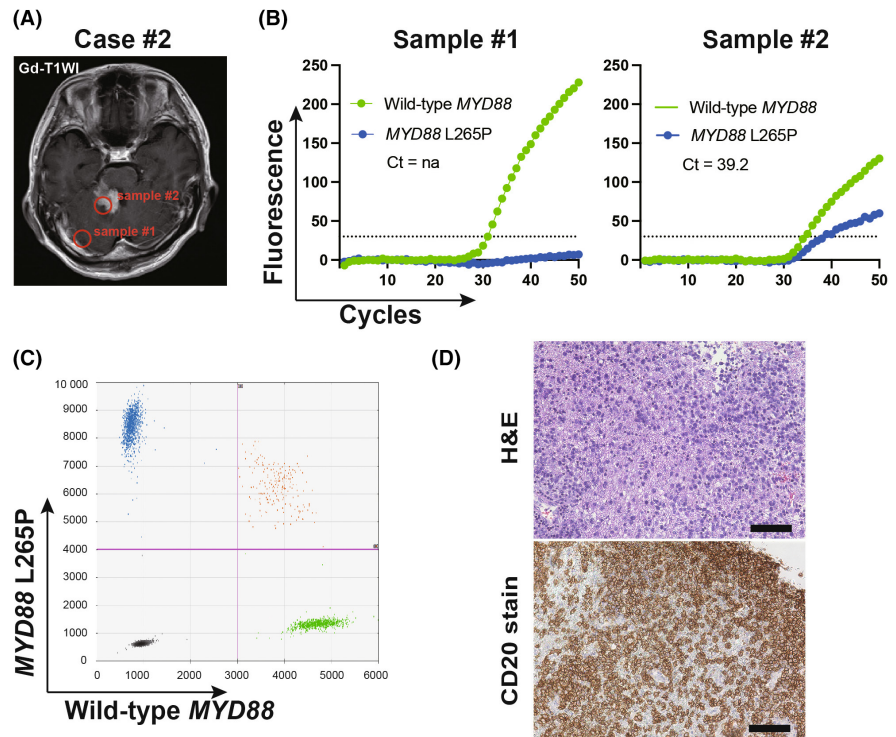
converges to the *MYD88* L265P mutation rate (64.0%–81.0%). As a result, the sensitivity of detection of the *MYD88* L265P mutation for intra-operative diagnosis of PCNSL is inferior to R-IHC and iFC. However, the detection of the *MYD88* L265P mutation is superior to these methods in terms of specificity (100%). Recently, based on data obtained from comprehensive studies, many CNS tumors, such as diffuse gliomas, which are one of the most frequent CNS tumors, are divided into several subgroups based on their genetic alterations, including *IDH* gene mutation.[20] Therefore, genotyping of the *MYD88* gene might align with the recent trend of diagnostics adopted in other brain tumors, such as glioma. Furthermore, detection of the *MYD88* L265P mutation using GeneSoC could be completed rapidly with a simpler technique that can be completed in the operating room. Intra-operative detection of the *MYD88* L265P mutation using GeneSoC contributes to improved accuracy of the intra-operative diagnosis of PCNSL, which minimizes surgical invasion and is beneficial. Notably, GeneSoC detected the *MYD88* L265P mutation in samples with as low as a 5% proportion of the *MYD88* L265P fragment, which serves as a limitation. GeneSoC can result in false-negative determination in samples with very low VAF. However, the VAF of gDNA derived from the biopsy sample was rarely less than 5%. Further, Hattori et al. reported a median VAF of 48.5% (10.5%–87%) in their PCNSL case series.[14] Our analyses of 24 cases using GeneSoC revealed no false negatives. However, it should be noted that when the *MYD88* L265P mutation is not detected by GeneSoC intra-operatively, PCNSL is not ruled out. Instead, ineligible collected samples for PCNSL with the wild-type *MYD88* and other tumors and inflammatory diseases should be considered, requiring intra-operative pathological examination to be referenced and samples collected again if necessary.

Primary central nervous system lymphoma sometimes develops from deep and eloquent areas where biopsy procedures might worsen neurological functions. Additionally, PCNSL tends to develop in elderly people who are less tolerant of surgical invasion. The definitive diagnosis of PCNSL without surgery could be beneficial for a subset of PCNSL cases. Liquid biopsy has been employed to detect the *MYD88* L265P mutation in cfDNA derived from CSF or plasma. As the VAF of the *MYD88* L265P mutation in cfDNA derived from plasma is very low, with a median of 0.34% (0.1%–0.69%), a highly sensitive assay, such as ddPCR, is considered to be necessary to detect the *MYD88* L265P mutation. Therefore, the *MYD88* L265P mutation was detected using the cfDNA of plasma at a frequency of just 20.0%–54.1% of PCNSL cases harboring the *MYD88* L265P mutation.[13,14,21] Accordingly, it was still considered insufficient as a marker for liquid biopsy due to its low sensitivity. In contrast, the VAF of the *MYD88* L265P mutation in cfDNA derived from CSF was not as low, which would warrant the use of ddPCR. Further, the detection sensitivity of GeneSoC was considered sufficient. Although ddPCR is more sensitive and requires the same amount of gDNA as GeneSoC, even at 0.5% VAF, the reduced processing, ease of manipulation, and faster analysis (approximately 15 min for GeneSoC vs. 3 h for ddPCR) make GeneSoC superior for use in the clinical setting. The *MYD88* L265P mutations are recognized in several lymphoproliferative diseases, and using these mutations for the diagnosis of PCNSL by liquid biopsy of the CSF is controversial. However, the usefulness of *MYD88* L265P mutation detection in cfDNA derived from CSF by ddPCR for a less-invasive diagnosis of PCNSL has been reported.[12,13] We showed that GeneSoC might be useful for detecting the *MYD88* L265P in cfDNA derived from CSF. In the
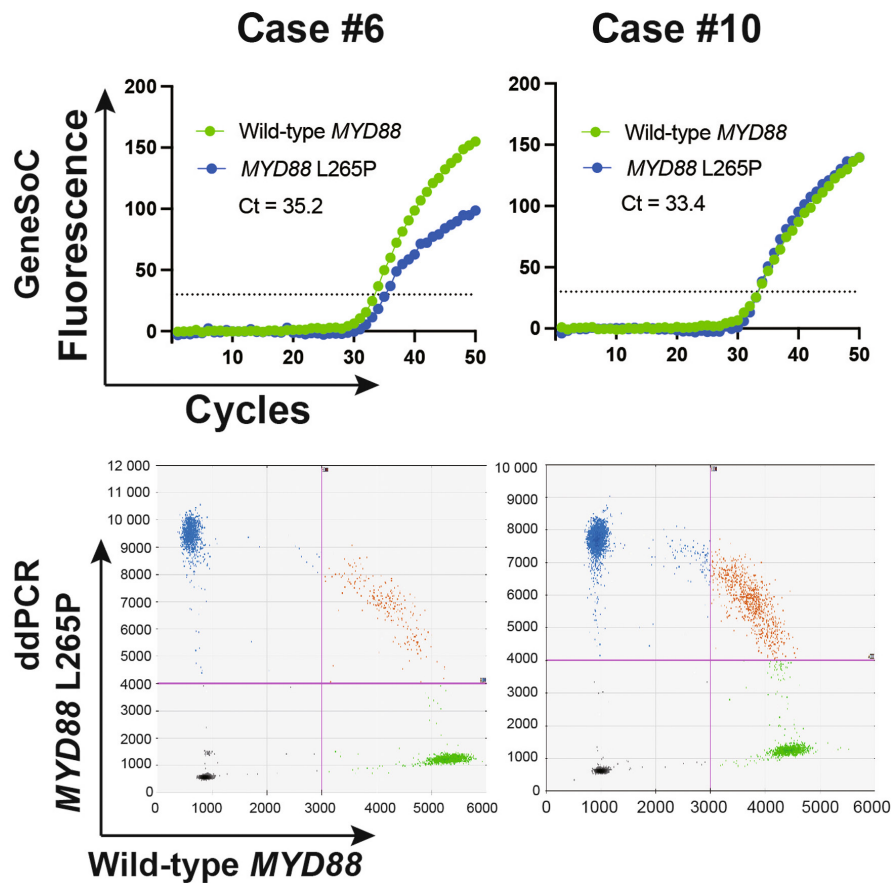
FIGURE 4 Clinical cases (Case #6 & #10) in which the *MYD88* L265P mutation was detected using cfDNA of cerebrospinal fluid using GeneSoC. The result of GeneSoC is shown in the upper row. The dotted line indicates the fluorescence threshold (30). The result of ddPCR is shown in the lower row. The pink line indicates the threshold (FAM; 4000, HEX; 3000).

future, a liquid biopsy of CSF may be combined with other clinical information to diagnose PCNSL.

In conclusion, genotyping by real-time PCR based on microfluidic thermal cycling technology enabled rapid detection of the *MYD88* L265P mutation, which helped improve intra-operative diagnosis of PCNSL and could be applied for future pre-operative diagnosis.

CONFLICT OF INTEREST STATEMENT

The study was conducted by Kyorin Pharmaceutical.

ETHICS STATEMENT

This study was performed in accordance with the principles of the Declaration of Helsinki. Approval was granted by the Institutional Review Board at Nagoya University Hospital (approval number: 2022–0043). Informed consent was obtained from all participants. Registry and the Registration No. of the study/trial are N/A. Animal Studies are N/A.

ORCID

Junya Yamaguchi https://orcid.org/0000-0002-4344-5750
Fumiharu Ohka https://orcid.org/0000-0002-5569-5626
Keiko Shinjo https://orcid.org/0000-0002-7797-6453
Yutaka Kondo https://orcid.org/0000-0003-3746-3191

REFERENCE

1. Zhou Y, Liu W, Xu Z, et al. Analysis of genomic alteration in primary central nervous system lymphoma and the expression of some related genes. *Neoplasia.* 2018;20(10):1059-1069. doi:10.1016/j.neo.2018.08.012
2. Takashima Y, Sasaki Y, Hayano A, et al. Target amplicon exomesequencing identifies promising diagnosis and prognostic markers involved in RTK-RAS and PI3K-AKT signaling as central oncopathways in primary central nervous system lymphoma. *Oncotarget.* 2018;9(44):27471-27486. doi:10.18632/oncotarget.25463
3. Nakamura T, Tateishi K, Niwa T, et al. Recurrent mutations of CD79B and MYD88 are the hallmark of primary central nervous system lymphomas. *Neuropathol Appl Neurobiol.* 2016;42(3):279-290. doi:10.1111/nan.12259

4. Fukumura K, Kawazu M, Kojima S, et al. Genomic characterization of primary central nervous system lymphoma. *Acta Neuropathol.* 2016;131(6):865-875. doi:10.1007/s00401-016-1536-2

5. Reddy A, Zhang J, Davis NS, et al. Genetic and functional drivers of diffuse large B cell lymphoma. *Cell.* 2017;171(2):481-494.e15. doi:10.1016/j.cell.2017.09.027

6. Lohr JG, Stojanov P, Lawrence MS, et al. Discovery and prioritization of somatic mutations in diffuse large B-cell lymphoma (DLBCL) by whole-exome sequencing. *Proc Natl Acad Sci USA.* 2012;109(10):3879-3884. doi:10.1073/pnas.1121343109

7. Chapuy B, Stewart C, Dunford AJ, et al. Molecular subtypes of diffuse large B cell lymphoma are associated with distinct pathogenic mechanisms and outcomes. *Nat Med.* 2018;24(5):679-690. doi:10.1038/s41591-018-0016-8

8. Brennan CW, Verhaak RG, McKenna A, et al. The somatic genomic landscape of glioblastoma. *Cell.* 2013;155(2):462-477. doi:10.1016/j.cell.2013.09.034

9. Paramasivam N, Hübschmann D, Toprak UH, et al. Mutational patterns and regulatory networks in epigenetic subgroups of meningioma. *Acta Neuropathol.* 2019;138(2):295-308. doi:10.1007/s00401-019-02008-w

10. Jonsson P, Lin AL, Young RJ, et al. Genomic correlates of disease progression and treatment response in prospectively characterized gliomas. *Clin Cancer Res.* 2019;25(18):5537-5547. doi:10.1158/1078-0432.Ccr-19-0032

11. Jones DT, Jäger N, Kool M, et al. Dissecting the genomic complexity underlying medulloblastoma. *Nature.* 2012;488(7409):100-105. doi:10.1038/nature11284

12. Yamagishi Y, Sasaki N, Nakano Y, et al. Liquid biopsy of cerebrospinal fluid for MYD88 L265P mutation is useful for diagnosis of central nervous system lymphoma. *Cancer Sci.* 2021;112(11):4702-4710. doi:10.1111/cas.15133

13. Hiemcke-Jiwa LS, Leguit RJ, Snijders TJ, et al. MYD88 p.(L265P) detection on cell-free DNA in liquid biopsies of patients with primary central nervous system lymphoma. *Br J Haematol.* 2019;185(5):974-977. doi:10.1111/bjh.15674

14. Hattori K, Sakata-Yanagimoto M, Suehara Y, et al. Clinical significance of disease-specific MYD88 mutations in circulating DNA in primary central nervous system lymphoma. *Cancer Sci.* 2018;109(1):225-230. doi:10.1111/cas.13450

15. Furutani S, Naruishi N, Hagihara Y, Nagai H. Development of an on-site rapid real-time polymerase chain reaction system and the characterization of suitable DNA polymerases for TaqMan probe technology. *Anal Bioanal Chem.* 2016;408(20):5641-5649. doi:10.1007/s00216-016-9668-8

16. Sugita Y, Terasaki M, Nakashima S, Ohshima K, Morioka M, Abe H. Intraoperative rapid diagnosis of primary central nervous system lymphomas: advantages and pitfalls. *Neuropathology.* 2014;34(5):438-445. doi:10.1111/neup.12126

17. Tanino M, Sasajima T, Nanjo H, et al. Rapid immunohistochemistry based on alternating current electric field for intraoperative diagnosis of brain tumors. *Brain Tumor Pathol.* 2015;32(1):12-19. doi:10.1007/s10014-014-0188-y

18. Malone H, Yang J, Hershman DL, Wright JD, Bruce JN, Neugut AI. Complications following stereotactic needle biopsy of intracranial tumors. *World Neurosurg.* 2015;84(4):1084-1089. doi:10.1016/j.wneu.2015.05.025

19. Koriyama S, Nitta M, Shioyama T, et al. Intraoperative flow cytometry enables the differentiation of primary central nervous system lymphoma from glioblastoma. *World Neurosurg.* 2018;112:e261-e268. doi:10.1016/j.wneu.2018.01.033

20. Louis DN, Perry A, Wesseling P, et al. The 2021 WHO classification of tumors of the central nervous system: a summary. *Neuro Oncol.* 2021;23(8):1231-1251. doi:10.1093/neuonc/noab106

21. Fontanilles M, Marguet F, Bohers É, et al. Non-invasive detection of somatic mutations using next-generation sequencing in primary central nervous system lymphoma. *Oncotarget.* 2017;8(29):48157-48168. doi:10.18632/oncotarget.18325

SUPPORTING INFORMATION

Additional supporting information can be found online in the Supporting Information section at the end of this article.